Biogeochemistry (2012) 110:183–200
DOI 10.1007/s10533-011-9698-4

Macroscale patterns of the biological cycling of dimethylsulfoniopropionate (DMSP) and dimethylsulfide (DMS) in the Northwest Atlantic

Martine Lizotte · Maurice Levasseur · Sonia Michaud · Michael G. Scarratt · Anissa Merzouk · Michel Gosselin · Julien Pommier · Richard B. Rivkin · Ronald P. Kiene

Received: 15 March 2011 / Accepted: 29 December 2011 / Published online: 14 January 2012

Abstract The influence of the seasonal development of microplankton communities on the cycling of dimethylsulfide (DMS) and its precursor dimethylsulfoniopropionate (DMSP) was investigated along a South–North gradient (36–59°N) in the Northwest (NW) Atlantic Ocean. Three surveys allowed the sampling of surface mixed layer (SML) waters at stations extending from the subtropical gyre to the Greenland Current during May, July and October 2003. Pools and transformation rates of DMSP and DMS were quantified and related to prevailing physical and biochemical conditions, phytoplankton abundance and taxonomic composition, as well as bacterioplankton abundance and leucine uptake. The South–North progression of the diatom bloom, a prominent feature in the NW Atlantic, did not influence the production of DMS whereas conditions in the N Atlantic Drift lead to a persistent bloom of DMSP-rich flagellate-dominated phytoplankton community and high net DMS production rates. Macroscale patterns of the observed variables were further explored using principal component analysis (PCA). The first axis of the PCA showed a strong association between the spatio-temporal distribution of DMSP and the abundance of several phytoplankton groups including dinoflagellates and prymnesiophytes, as well as with microbial-mediated $DMSP_d$ consumption and yields and rates of the conversion of DMSP into DMS. The second axis revealed a strong association between concentrations of DMS and SML depth and photosynthetically active radiation, a result supporting the prominent role of solar radiation as a driver of DMS dynamics.

Keywords Dimethylsulfide (DMS) · Dimethylsulfoniopropionate (DMSP) · Bacteria · Phytoplankton · Solar radiation · Sulfur cycling · North Atlantic

M. Lizotte (✉) · M. Levasseur · A. Merzouk
Département de biologie, Québec-Océan, Université Laval, Quebec, QC G1V 0A6, Canada
e-mail: martine.lizotte@qo.ulaval.ca

S. Michaud · M. G. Scarratt
Fisheries and Oceans Canada, Maurice Lamontagne Institute, Mont-Joli, QC G5H 3Z4, Canada

M. Gosselin
Institut des sciences de la mer de Rimouski, Université du Québec à Rimouski, 310 Allée des Ursulines, Rimouski, QC G5L 3A1, Canada

J. Pommier
Laboratoire de Radioécologie de Cherbourg-Octeville, Institut de Radioprotection et de Sureté Nucléaire, Cherbourg-Octeville 50130, France

R. B. Rivkin
Ocean Sciences Center, Memorial University of Newfoundland, St-John's, NF A1C 5S7, Canada

R. P. Kiene
Department of Marine Sciences, University of South Alabama, Mobile, AL 36688, USA

Introduction

Dimethylsulfide (DMS) produced by marine microbiota is the dominant volatile sulfur (S) compound in surface waters of the oceans (Lovelock et al. 1972). In the atmosphere, DMS is oxidized into various products including submicron-size sulfate and sulfonate particles which contribute to atmospheric acidity and aerosols (Andreae and Crutzen 1997). The latter scatter solar radiation and act as efficient cloud condensation nuclei (CCN), thereby potentially modifying cloud microphysics and albedo, and influencing the radiation budget of the Earth (Charlson et al. 1987; Andreae and Rosenfeld 2008). Because the rate of sea-to-air DMS emission is driven by its concentration in the surface ocean, there has been extensive work on identifying and quantifying the processes that control the production and loss of DMS within the marine plankton community with the ultimate goal being the prediction of DMS emissions as a function of region and time. Seasonal field studies and data compilation of oceanic DMS concentrations have shown large variability in average surface seawater DMS concentrations that vary by 50-fold between winter and summer in mid- to high-latitudes (i.e. 0.2 nmol l^{-1} in winter and 10 nmol l^{-1} in summer, see Lana et al. 2011 and references cited therein).

Understanding the temporal and spatial variability of DMS concentrations in the surface mixed layer (SML) requires that concentrations and turnover processes of its precursor, the microalgal metabolite dimethylsulfoniopropionate (DMSP), be determined over relevant spatial and temporal scales. Intracellular concentrations and cycling of DMSP vary among phytoplankton taxa. Eukaryotic micro- and nanophytoplankton such as dinoflagellates and prymnesiophytes often dominate DMSP production in oceanic environments, but other groups including diatoms, prasinophytes, chrysophytes and cryptophytes (Keller et al. 1989), as well as picoeukaryotes and cyanobacteria, such as Synechoccus spp., may contain significant amounts of DMSP (Archer et al. 2011), likely through uptake and retention of DMSP for the latter group (Malmstrom et al. 2005). Algal DMSP is produced as a response to multiple environmental forcings (Simó 2004 and references cited therein) and part of the intracellular pool of DMSP may be released into seawater through exudation, grazing, viral attack and autolysis (Stefels 2000; Simó 2001). Production of DMS results from the enzymatic cleavage of DMSP either from the dissolved pool ($DMSP_d$) in bulk seawater or directly from the particulate pool ($DMSP_p$) via bacterial or algal DMSP-lyases (Stefels 2000, Stefels et al. 2007; Yoch 2002). The efficiency of bacterial conversion of DMSP into DMS may vary from 2 to 100% depending on the nutrient status of bacteria and the quantity and quality of the pool of dissolved organic matter (Kiene et al. 2000). The direct production of DMS via algal DMSP-lyase enzymes has been related to phytoplankton speciation and physiological status as well as to environmental stressors, while indirect DMS production may occur following cellular lysis and concurrent mixing of algal DMSP-lyases with the $DMSP_d$ reservoir [see review by Stefels et al. (2007)]. The cycling of DMSP and its degradation products is thus intimately linked with food web processes in the surface ocean where microbial communities play a central role (Kiene et al. 2000; Stefels et al. 2007).

The North (N) Atlantic Ocean is recognized as one of the most productive regions of the World Ocean in terms of DMS concentrations, with seasonal averages over 10 nmol l^{-1} in some areas (Lana et al. 2011). Surveys conducted in the Northwest (NW) Atlantic have shown that the spatial and temporal progression of phytoplankton blooms is important in controlling the distribution of DMS (Scarratt et al. 2000b, 2002, 2007; Lizotte et al. 2008). In the polar and subpolar regions of the N Atlantic, results from a macroscale DMS data compilation study (Lana et al. 2011 and references therein) reveal the presence of a pronounced DMS seasonal cycle with increasing DMS concentrations in summer coupled to increases in phytoplankton biomass. While, in the temperate low-latitude and northern subtropical regions of the N Atlantic, the seasonal pattern shows a decoupling between concentrations of DMS and phytoplankton biomass during summer, a feature identified as the 'summer paradox' (Simó and Pedrós-Alió 1999). However, beyond what is known from the Sargasso Sea, where complete annual cycles have been reported (Dacey et al. 1998), our understanding of the seasonal variations in DMS production in other biogeochemical provinces of the N Atlantic relies on a combination of data collected in different months/seasons during different years. Although useful, these seasonal 'reconstructions' limit our appreciation of the mechanisms responsible for the seasonal evolution of the

DMS(P) dynamics and how they are inter-related in time and space.

During spring, summer and fall of the year 2003, we followed the seasonal and meridional development of the annual phytoplankton bloom and characterized the distribution and microbial dynamics of pools of DMS and DMSP in seven distinct biogeochemical provinces of the NW Atlantic. Moreover, we explored the meridional extent of the mismatch between the distribution of phytoplankton biomass and concentrations of DMS described at low latitudes and referred to as the 'summer paradox'.

Materials and methods

Oceanographic setting

Eight stations were occupied between 36°55′N and 59°34′N in the NW Atlantic Ocean as part of the Canadian Surface Ocean—Lower Atmosphere Study (SOLAS) expeditions in May (01–10) aboard CCGS *Hudson*, July (08–22) and October (13–27) 2003 aboard CCGS *Martha L. Black* (Fig. 1). The biogeochemical province designation of the stations were a posteriori assigned following a dynamic method of physical and biological categorization of ocean regions using ocean color radiometry of both sea surface temperature and chlorophyll *a* (chl *a*) concentration developed by Devred et al. (2007). The use of this dynamic method for the ecological partitioning of the NW Atlantic avoids the limitations that arise from static boundaries, which do not take into account variations in ocean circulation (hence water masses) following seasonal cycles or in response to intense atmospheric events (Longhurst et al. 1995; Longhurst 2006; Platt and Sathyendranath 1999). Biogeochemical province boundaries changed from spring to fall 2003 (Table 1).

Field sampling

Vertical profiles of salinity and temperature were determined using a Conductivity Temperature Depth (CTD) probe (Sea-Bird SBE 9/11 plus) mounted on a rosette sampler. Seawater samples for the determination of extracted chl *a*, DMSP and DMS concentrations, phytoplankton and bacteria, and rate processes were collected within the SML (depth range: 8–15 m) with 10-l Niskin-type bottles. Water samples for the determination of pools and transformations rates of DMSP and DMS were pre-screened on a 210-μm Nitex mesh to remove large grazers.

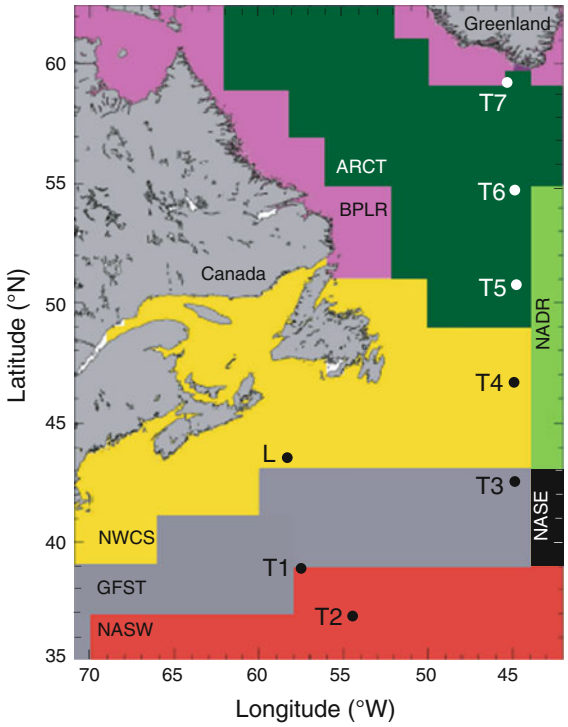

Fig. 1 Location of the eight sampling stations in the Northwest Atlantic Ocean within static biogeochemical province boundaries according to Longhurst (2006): North Atlantic Subtropical Gyral West and East (NASW and NASE, respectively); Gulf Stream (GFST); Northwest Continental Shelves (NWCS); North Atlantic Drift (NADR); Atlantic Arctic (ARCT); Boreal-Polar (BPLR; not sampled)

Solar irradiance and wind speed

At each station, a vertical profile of irradiance (incident photosynthetically active radiation: PAR, 400–700 nm) was measured with a PNF-300 radiometer (Biospherical Instruments). The downwelling irradiance was also measured during each cruise at 5 min intervals during spring and at 10 min intervals during summer and fall using a LI-COR 2 π PAR sensor (model LI-190SA quantum sensor). The downwelling irradiance values ($\mu E\ m^{-2}\ s^{-1}$) were averaged over 24-h and converted to radiometric units ($W\ m^{-2}$) by dividing measurements by a factor of 4.6. To further investigate a potential relationship between irradiance and DMS concentrations, we calculated the

Table 1 Geographic coordinates and corresponding biogeochemical province of the eight stations sampled during spring, summer and fall 2003 in the NW Atlantic Ocean determined from a dynamic delineation (Devred et al. 2007)

Station	Latitude	Longitude	Dynamic biogeochemical province		
	(N)	(W)	Spring	Summer	Fall
T2	36°5′	54°4′	NASE	NASW	NASW
T1	39°0′	57°3′	GFST	NASW	GFST
T3	42°2′	45°0′	SW	SW	NASE
L	43°3′	57°3′	NWCS	SW	SW
T4	46°3′	45°0′	NADR	NADR	NADR
T5	50°4′	45°0′	NADR	NADR	NADR
T6	54°5′	45°0′	ARCT	ARCT	NADR
T7	59°2′	45°0′	n.a.	ARCT	ARCT

The three cruises encompassed provinces from the Polar biome: Atlantic Arctic (ARCT); the Westerlies biome: North Atlantic Subtropical Gyre West and East (NASW and NASE, respectively), Gulf Stream (GFST), North Atlantic Drift (NADR); the Coastal biome: Northwest Continental Shelves (NWCS); and finally a new province with unique characteristics proposed by Devred et al. (2007), called the Slope Water (SW). This latter province represents a transition region between the warm oligotrophic waters (NASW, NASE and GFST) and the cooler, richer waters of the continental shelf

Information that is not available is noted as n.a

solar radiation dose (SRD in W m^{-2}) index of Vallina and Simó (2007) using Eq. 1:

$$\mathrm{SRD} = (\mathrm{E_o}/(\mathrm{k_d} \cdot \mathrm{SML})) \cdot \left(1 - e^{(-\mathrm{kd}\cdot\mathrm{SML})}\right) \quad (1)$$

where E_o is the daily averaged incident PAR (in W m^{-2}), k_d is the diffuse attenuation coefficient (m^{-1}) determined from the PAR profiles as the slope of an ordinary least squares (OLS) regression between the ln-transformed downwelling irradiance and the depth, and SML (m) is the depth at which sigma t was 0.125 kg m^{-3} higher than that at the surface (Levitus 1982), using 10 m during spring and 5 m during summer and fall as the surface references. A coarser SML criterion was used because of its greater likelihood to capture seasonal mixed layers that could possibly reflect succession-derived features rather than recent light history, as this aspect is partly being captured through measurements of daily-averaged incident PAR. Note that in Vallina and Simó (2007), E_o represents the total shortwave radiation (ca. 300–3,000 nm). Here, the SRD index indicates the average daily PAR in the SML. Wind speed (knots) was recorded every 4 h with the ship's on-board system, averaged over 24 h and converted to m s^{-1}

Table 2 Seasonal average (range) of physical characteristics (daily averaged wind speed, SML depth, daily averaged PAR, diffuse attenuation coefficient (k_d) and SRD), and DMSP-cycling ratios ($DMSP_t$:Chl *a*, DMS:Chl *a*, DMS:$DMSP_t$, DMS production from $DMSP_d$ normalized over $DMSP_t$, DMS production from $DMSP_t$ normalized over $DMSP_t$) measured at each station along a meridional transect in the NW Atlantic Ocean in spring, summer and fall 2003

	Spring	Summer	Fall
Physical properties			
Wind speed (m s^{-1})	7.6 (3–19)	5.1 (2–8)	12.5 (5–19)
SML depth (m)	76 (23–218)	13 (8–29)	45 (12–70)
PAR (W m^{-2})	91 (58–120)	96 (66–143)	42 (13–87)
k_d (m^{-1})	0.07 (0.05–0.14)	0.07 (0.03–0.10)	0.08 (0.06–0.12)
SRD (W m^{-2})	24 (6–41)	68 (41–106)	13 (4–29)
DMSP-cycling			
$DMSP_t$:Chl *a* (nmol μg^{-1})	26 (5–52)	88 (24–168)	41 (9–92)
DMS:Chl *a* (nmol μg^{-1})	1.3 (0.3–3.9)	10.6 (0.7–29.3)	1.3 (0.2–3.4)
DMS:$DMSP_t$ (mol mol^{-1})	0.05 (0.01–0.11)	0.21 (0.02–1.19)	0.03 (0.01–0.07)
DMS prod from $DMSP_d$:$DMSP_t$ (day^{-1})	0.02 (0.01–0.04)	0.02 (0.01–0.06)	0.02 (0.01–0.03)
DMS prod from $DMSP_t$:$DMSP_t$ (day^{-1})	0.04 (0.02–0.08)	0.06 (0.02–0.08)	0.07 (0.02–0.21)

Number of observations: $n = 7$ in spring and $n = 8$ in summer and fall

(see Table 2 for seasonal averages and ranges of physical characteristics).

Nutrients, chlorophyll *a* analysis and phytoplankton enumeration

Samples for dissolved inorganic nutrients were collected in the SML and filtered through precombusted (450°C for 5 h) Whatman GF/F glass fiber filters (nominal pore size of 0.7 μm). The filtrate was immediately frozen at −80°C in acid-cleaned polypropylene cryovials and processed within 2 months for the determination of nitrate + nitrite ($NO_3^- + NO_2^-$) using an Alpkem FS III autoanalyzer. Coefficients of variation (CV) for duplicate samples of $NO_3^- + NO_2^-$ were <1%. Concentrations of chl *a* were measured aboard the ship following the fluorometric method of Parsons et al. (1984) described in detail in Pommier et al. (2008). Phytoplankton samples were fixed and preserved in hexamine-buffered formaldehyde (for calcified Prymnesiophytes) and in acidic Lugol's solution (for the other algal groups including non-calcified Prymnesiophytes) for later identification and enumeration using the inverted microscope method (Utermöhl 1931). An important limitation of the cell count technique used in this study is the poor characterization it offers of the picoplankton community, both the prokaryotic component, commonly dominated by Prochlorococcus and Synechococcus, as well as the eukaryotic fraction. Various species within the picophytoplankton have been shown to play diverse roles in DMS(P) cycling, as producers but also consumers of DMSP (Malmstrom et al. 2005; Vila-Costa et al. 2006).

Bacterial abundance and leucine incorporation rates (LIR)

Samples for the determination of bacterioplankton abundance were preserved with borate-buffered formaldehyde (2% final concentration) and kept in 20 ml scintillation vials in the dark at 4°C. For the enumeration of bacteria, two to three ml subsamples were filtered onto 0.2 μm pore-size black polycarbonate membranes (Costar), stained with DAPI, and counted with an epifluorescence microscope (Porter and Feig 1980) within 4 weeks of sample collection. The average CV (<11%) for bacterial abundance was determined from 20 replicate fields of view per filter. In the current study, "bacteria" refers to the bulk microbial community, including Archaea, since the microscopic technique used for their enumeration does not allow any differentiation of microbial assemblages. Rates of bacterial [^{14}C]-leucine incorporation were estimated from 4 to 6 h dark incubations in sterile test tubes, at ambient water temperatures following standard protocols (Kirchman and Ducklow 1993). The average CV of [^{14}C]-LIR for triplicate samples was ca. 10%. Protocols for the determination of leucine incorporation were not customized for the different trophic environments encountered during our extensive study. As a result, an underestimation of the rates is not excluded especially in highly productive waters where kinetics of leucine incorporation may saturate after only a few hours.

Analysis of methylated S compounds

Concentrations of $DMSP_p$, $DMSP_d$ and DMS were determined following procedures described by Scarratt et al. (2000a) and Lizotte et al. (2008) using purging, cryotrapping and S-specific gas chromatography (GC). Seawater samples (71-ml) were gravity filtered through 47-mm Whatman GF/F filters. The filtrate was used to determine concentrations of both DMS and $DMSP_d$. Samples of DMS were analyzed on board the ship within a few minutes of sampling while $DMSP_d$ + DMS samples were subjected to alkali treatment (KOH, 0.4 mol l^{-1} final concentration), sealed in 24-ml serum vials and stored for future analysis. Concentrations of $DMSP_p$ were determined by placing the filter in a solution of KOH (0.4 mol l^{-1} final concentration) and processing samples as described above for $DMSP_d$. All DMSP samples were kept in the dark at 4°C for at least 24 h and analyzed within a week of collection. Concentrations of $DMSP_d$ were calculated by subtracting DMS from $DMSP_d$ + DMS while concentrations of total DMSP ($DMSP_t$) were calculated by adding values of $DMSP_d$ and $DMSP_p$. Values of $DMSP_d$ concentrations should be considered with caution in view of the recent demonstration that the common filtration procedure may result in spurious release of DMSP from phytoplankton cells, resulting in an overestimation of $DMSP_d$ concentrations (Archer et al. 2002; Kiene and Slezak 2006). In this study, the same filtration procedure was used in all three cruises and 91% of our values fall in the 0.3–4.7 nmol l^{-1} range which is comparable to the range of $DMSP_d$ concentrations (0.4–2.8 nmol l^{-1}) measured using a less

disruptive filtration method (small volume drip filtration—SVDF, see Kiene and Slezak 2006).

Subsamples of DMSP and DMS were withdrawn from the sample vials and sparged using a purge and trap system coupled to a Varian 3400 or 3800 GC equipped with a pulsed flame photometric detector (PFPD) (see Scarratt et al. 2000a for details). For the analysis of DMSP, the GC was calibrated with milliliter injections of a 5 μg ml^{-1} solution of hydrolyzed DMSP (Research Plus Inc.). DMS samples were calibrated with microliter injections of DMS diluted with ultra high purity grade helium prepared using a permeation tube (Certified Calibration by Kin-Tek Laboratories Inc.) maintained at 40°C. The analytical precision (CV) for triplicate measurements of DMSP and DMS was better than 10%.

Shipboard incubations for the determination of microbial DMSP and DMS metabolism

Two types of incubations were undertaken simultaneously to measure transformation rates of DMSP and production rates of DMS. Microplankton community net DMS production and microbial net DMS production are referred to as DMS production from $DMSP_t$ and DMS production from $DMSP_d$, respectively, following the nomenclature of Slezak et al. (2007).

For the determination of rates of net DMS production from $DMSP_t$, duplicate samples of seawater were collected in the SML, transferred in gas-tight 1-L Tedlar bags (Chromatographic Specialties Inc.), and incubated in the dark at in situ water temperature. Subsamples were withdrawn at time 0, 3, and 6-h following a gentle mixing of the bags. At each time point, the subsamples (71 ml) were processed and analyzed for DMS concentrations, as described above. Production rates of DMS (nmol DMS l^{-1} day^{-1}) were estimated from the slope of the change in the concentrations of DMS over the 6-h incubation period (Model I linear regression). The average for absolute deviations in duplicate measurements of DMS production rates from $DMSP_t$ was 9%. Inhibitors of the bacterial consumption of DMS were not used during these incubations thus reported rates represent net biological production of DMS (gross production minus consumption). Furthermore, rates of DMS production from $DMSP_t$ are considered to represent the production of DMS by the microplankton community, i.e. the net sum of DMS producing pathways mediated by bacterioplankton, phytoplankton, and microzooplankton smaller than 210 μm. As a result, potential indirect production of DMS following mesozooplankton activity is not considered here.

For the determination of rates of DMS production from $DMSP_d$, SML seawater samples were collected in 71 ml brown polyethylene bottles and amended with ^{35}S-$DMSP_d$ at tracer concentrations (<0.01 nmol l^{-1}) following protocols described in Kiene and Linn (2000b). Samples were incubated in the dark at in situ water temperature over a 3-h period. Total amount of isotope added was determined following the addition of ^{35}S-DMSP. Subsamples were taken at time 0, 0.5, 1, and 3-h in order to determine the amount of ^{35}S recovered into volatiles as well as unreacted ^{35}S-DMSP following methods described hereafter. The amount of DMS produced from bacterial $DMSP_d$ degradation at each time point was determined in 5 ml subsamples after addition of sodium dodecyl sulfate (SDS, 0.2% final concentration) and cold $DMSP_d$ (100 μmol l^{-1} final concentration) to stop further reaction of ^{35}S-$DMSP_d$. Radio labeled volatiles, including ^{35}S-DMS and ^{35}S-methanethiol (MeSH), were trapped in 3% H_2O_2-soaked wicks during a 6-h shaking period. The wicks were transferred to 10 ml CytoScint and stored in the dark for further analysis. Unconsumed ^{35}S-DMSP was converted into ^{35}S-volatiles by injection of 0.2 ml of NaOH (5 mol l^{-1}) into sealed vials and recovery of these ^{35}S-volatiles was conducted as described above. Although we cannot completely exclude the presence of MeSH in the pool of recovered ^{35}S-volatiles, we consider this pool to be mainly ^{35}S-DMS (Kiene and Linn 2000b). Finally, the amount of isotope in each sample was analyzed with a RackBeta scintillation counter (LKB Wallac) within a few weeks of collection.

These incubation experiments allowed the calculation of different rates. The $DMSP_d$ loss rate constant (k_{DMSPd} in day^{-1}) was estimated from the slope of the change in ln-transformed activity of unreacted ^{35}S-DMSP over the 3 h incubation period (Kiene and Linn 2000b). $DMSP_d$ consumption rates (nmol $DMSP_d$ l^{-1} day^{-1}) were obtained by multiplying the k_{DMSPd} by the concentrations of in situ $DMSP_d$. The DMS yield from $DMSP_d$ (%) was calculated as the ratio of ^{35}S-DMS recovered to ^{35}S-$DMSP_d$ consumed at the end of the 3-h incubations, expressed as a percentage. Rates of DMS production from $DMSP_d$ (nmol DMS l^{-1} day^{-1}) were estimated from the product of the $DMSP_d$

consumption rate and the DMS yield from $DMSP_d$. The experimental procedures for ^{35}S-DMSP incubations were conducted in duplicate on three occasions during the study period and the average of absolute deviations for estimates of $DMSP_d$ loss rate constants and DMS yields from $DMSP_d$ was <12%. Inhibitors of the bacterial consumption of DMS were not used in these incubations thus measured rates represent the net production (NP) of DMS (gross production minus consumption). Furthermore, as there is no evidence suggesting that $DMSP_d$-consuming phytoplankton such as diatoms (Vila-Costa et al. 2006) may cleave DMSP into DMS, we consider our DMS yields from $DMSP_d$ and rates of DMS production from $DMSP_d$ to be essentially bacterially-mediated. We do not, however, exclude the possibility of $DMSP_d$-to-DMS conversion via extracellular algal DMSP-lyases (Stefels 2000) in our ^{35}S-$DMSP_d$ tracer incubations and values shown here should be considered as upper limit measurements of DMS yields from $DMSP_d$ and production rates mediated by bacterioplankton.

Statistical analyses

Model I linear regressions were used to determine biological rates during incubations (Sokal and Rohlf 1995). A principal component analysis (PCA) was used to show the relationships among original variables and rates in the reduced space (Legendre and Legendre 1998). This ordination has been previously used to describe the role of water mass dynamics on DMSP cycling in the St. Lawrence Estuary (Michaud et al. 2007). The PCA was conducted on a correlation matrix composed of 22 variables and 23 data rows. The magnitude of multicolinearity within our dataset was analyzed by considering the size of the variance inflation factor (VIF) using Eq. 2:

$$\mathrm{VIF} = 1/\left(1 - r^2\right) \quad (2)$$

where r^2 is the coefficient of determination of the regression equation obtained by ordinary least squares regressions on paired variables. To minimize the effect of multicolinearity, variables which had a VIF > 5 were excluded from the PCA. Furthermore, only primary and methodologically independent variables were included in the PCA. Before performing the analysis, the data were log10-transformed and standardized, in order to normalize the distribution and harmonize differences in units and scales within observations, as recommended by Legendre and Legendre (1998). It is essential to state here that the PCA incorporates physicochemical and biological variables that are representative of wide ranging timescales. For instance, wind speed and incident PAR, which are averaged over 24 h, are combined with other physicochemical forcings, such as SML depth and concentrations of $NO_3^- + NO_2^-$, which integrate information over a much longer period of time. For this reason, only broad patterns and highly significant correlations that meet the threshold criteria of $p < 0.01$ are discussed. In order to facilitate ecological interpretation, the axes were submitted to a varimax orthogonal rotation. The circle of equilibrium descriptor contribution (EDC) was computed in order to indicate which variables contribute the most strongly to the reduced space by using Eq. 3:

$$\mathrm{EDC} = (d/p)^{0.5} \quad (3)$$

where d is the number of dimensions, and p is the number of descriptors. Accordingly, little information can be obtained for descriptors whose projections are inferior to the equilibrium contribution circle. Because projections of descriptor angles in a reduced space do not render the complete correlations between variables, Spearman's rank correlation coefficients (r_s) were used to evaluate the relationship between two variables following assessments of normality in data distributions using Kolmogorov–Smirnov tests. Statistical analyses were carried out using the Systat statistical software for Windows version 9, and Microsoft Office Excel 2003.

Results

Oceanographic conditions and phytoplankton-related variables

During the three sampling seasons, water temperature and salinity of the SML decreased with increasing latitude (Fig. 2a, b). Concentrations of $NO_3^- + NO_2^-$ increased with latitude during the three seasons, but we observed a marked decrease in $NO_3^- + NO_2^-$ concentrations during summer and fall at higher latitudes (Fig. 2c). At the lower latitudes, concentrations of chl *a* were highest in spring, while at the higher latitudes, concentrations of chl *a* were generally higher in summer than in spring and fall, reflecting the South–North progression of the bloom (Fig. 2d).

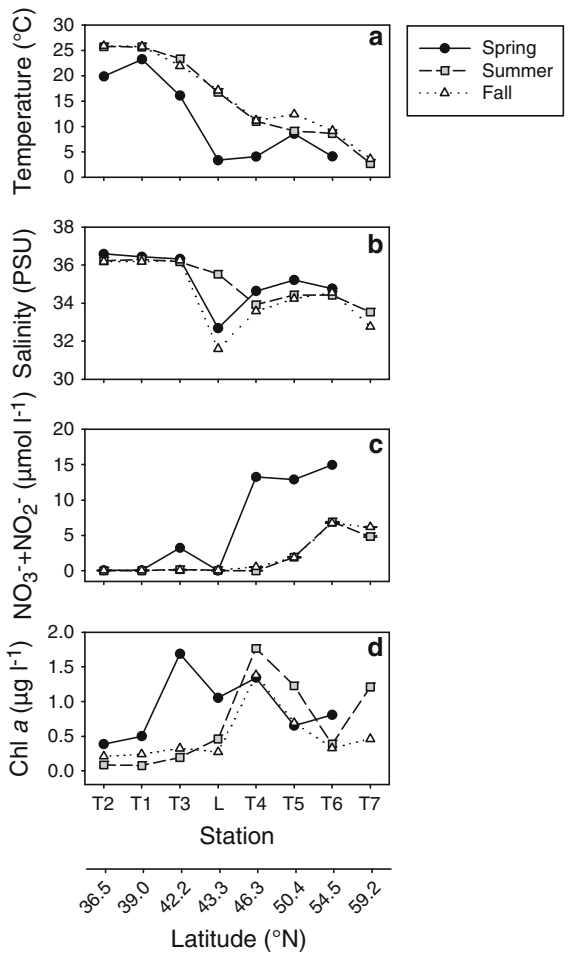

Fig. 2 Spatio-temporal variations of **a** temperature, **b** salinity, and **c** nitrate plus nitrite ($NO_3^- + NO_2^-$) concentration, and **d** chl *a* concentrations measured at one depth (8–15 m) in the SML

At the lower latitudes, diatom abundance was generally higher in spring (note Station T3, Fig. 3a) than in summer and fall, while at the higher latitudes, diatom abundance was generally higher in summer than in spring and fall. The spatial distribution of diatom abundance during fall was relatively uniform across the meridional transect. It is noteworthy that chl *a* concentrations were high at T4 in the North Atlantic Drift (NADR) during the three cruises, irrespective of the South–North progression of the diatom bloom and nitrate drawdown (Fig. 2c, d; Fig. 3a).

The spatial distribution of the abundance of prymnesiophytes was variable during spring, generally increased with latitude during summer and exhibited highest values at mid-latitude stations during fall (Fig. 3b). Dinoflagellate abundance was spatially variable during all three seasons with highest abundances measured at mid-latitudes (Fig. 3c).

Throughout seasons and stations, unidentified phytoplankton (specifically nanoflagellates 2–5 µm in size) generally dominated the assemblages in terms of abundance (Fig. 3d). The spatial distribution of flagellates was relatively constant during spring. Spatial trends of the abundance of flagellates during summer and fall were variable with highest values observed at the mid-latitude stations. In contrast, flagellate abundance was relatively similar between seasons at the lower latitudes.

The abundance of cryptophytes was low and constant throughout seasons at lower latitude stations (Fig. 3e) and displayed greater variability at mid- to high-latitude stations during all three seasons of investigation. The abundance of prasinophytes and chrysophytes was very low and relatively constant across stations during the entire sampling period (Fig. 3f, g, note differences in scale), exception made of station T4 which displayed a higher abundance of prasinophytes during summer.

Pools of methylated S compounds

Concentrations of $DMSP_p$ ranged from 4.2 to 101 nmol l^{-1} during the study period and displayed maximal concentrations at ca. 50°N during all three seasons (Fig. 4a). The distribution of $DMSP_d$ was relatively constant during spring, while concentrations of $DMSP_d$ were more spatially variable during summer and fall with highest values measured at the mid-latitudes (Fig. 4b). Concentrations of DMS varied between 0.11 and 11 nmol l^{-1} within the entire dataset (Fig. 4c). In general, concentrations of DMS showed much less spatial variability than pools of DMSP during all three seasons, with the exception of a high concentration of DMS at Station T6 during summer.

Microbial dynamics and metabolism of methylated S compounds

Overall, bacterial abundance ranged from 0.11×10^9 cells l^{-1} to 1.49×10^9 cells l^{-1} (Fig. 5a). Spatially, bacterial abundance was relatively uniform along the meridional transect, with the exception of high abundances observed around 45–50°N latitude during fall. Rates of bacterial leucine incorporation were

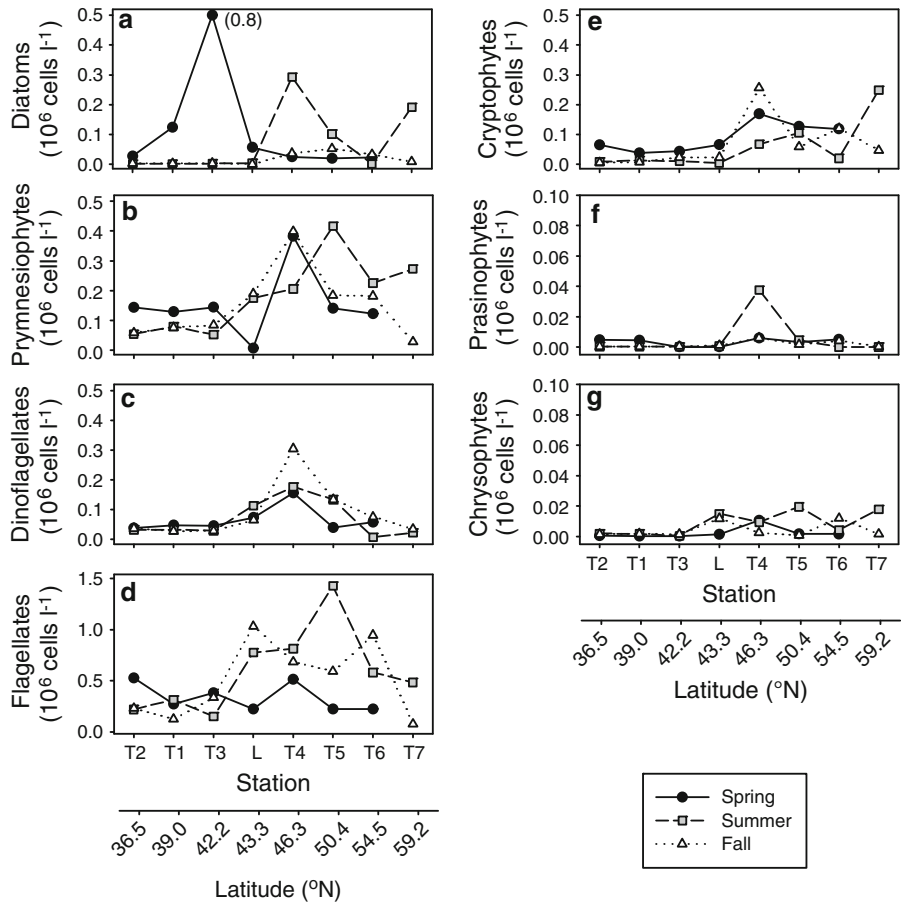

Fig. 3 Spatio-temporal variations in the abundance of **a** diatoms, **b** prymnesiophytes, **c** dinoflagellates, **d** unidentified flagellates, **e** cryptophytes, **f** prasinophytes, and **g** chrysophytes measured at one depth (8–15 m) in the SML

spatially variable in spring with highest rates measured between 40 and 45°N (up to 2.3 nmol Leu l^{-1} day^{-1} at station L, Fig. 5b). During summer, LIR exhibited spatial variations with highest rates measured in stations located from 45 to 55°N where maximum chl *a* concentrations were also observed. Bacterial LIR were low (<0.3 nmol Leu l^{-1} day^{-1}) and relatively constant throughout stations in fall.

Spring values of k_{DMSPd}, an indicator of the ability of the microbial assemblage to use $DMSP_d$, were generally similar across stations ranging between 1.4 and 2.6 day^{-1} (Fig. 5c). Spatial variability in k_{DMSPd} was greater during summer and fall with values ranging from 0.7 to 1.0 day^{-1} at T7 (during summer and fall, respectively) to 4.1 day^{-1} at T4 (during summer). $DMSP_d$ consumption rates varied between 0.3 and 24.3 nmol $DMSP_d$ l^{-1} day^{-1} (Fig. 5d). The spatial distribution in rates of $DMSP_d$ consumption was more variable during summer and fall than in spring, with highest values measured at Station T4.

Values of DMS yields ($DMSP_d$-to-DMS conversion efficiency) were generally higher in spring than in fall along the meridional transect (Fig. 5e). In summer, highest DMS yields from $DMSP_d$ were measured at stations located between 45 and 50°N. Overall, DMS yields from $DMSP_d$ varied between 3 and 21% over the entire period of investigation.

Rates of net DMS production from $DMSP_d$ were low and relatively stable between stations during spring ranging from 0.2 to 0.6 nmol DMS l^{-1} day^{-1} (Fig. 5f). High values (up to 3.1 nmol DMS l^{-1} day^{-1}) were measured at Station T4 in summer and fall. At mid-latitude, rates of net DMS production from $DMSP_d$ were highest in summer, while at the low- and high-latitude stations, rates of net DMS production from $DMSP_d$ were relatively similar

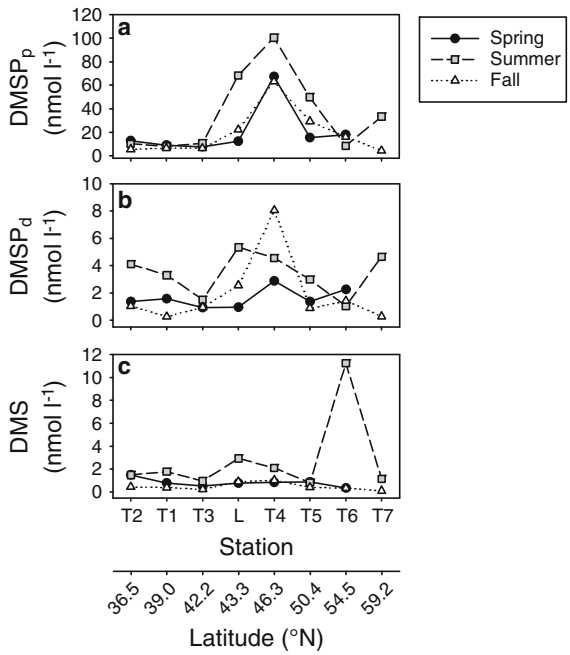

Fig. 4 Spatio-temporal variations of concentrations of **a** particulate $DMSP_p$, **b** dissolved $DMSP_d$, and **c** DMS measured at one depth (8–15 m) in the SML

between seasons. Net DMS production from $DMSP_t$ exhibited similar spatial and temporal patterns as the ones observed for net DMS production from $DMSP_d$ (Fig. 5g). Springtime was characterized by overall low net DMS production from $DMSP_t$. Highest values were measured at Station T4 during summer and fall with 4.9 and 4.3 nmol DMS l^{-1} day^{-1}, respectively.

Emergent properties of the system

Our dataset was subjected to a two-dimensional PCA (see Fig. 6), composed of 22 variables and 23 data rows. The PCA reveals that 56% of the total variation is accounted for by the first two principal components. Component scores for the first two orthogonal components (PC1 and PC2) were regressed against environmental, biological and microbial DMSP cycling-related variables. The main variables that significantly contribute to the formation of the PC1 are $DMSP_p$ ($r^2 = 0.86$, $p < 0.001$), dinoflagellates ($r^2 = 0.61$, $p < 0.001$), $DMSP_d$ ($r^2 = 0.54$, $p < 0.001$), flagellates ($r^2 = 0.53$, $p < 0.001$), net DMS production from $DMSP_t$ ($r^2 = 0.52$, $p < 0.001$), prasinophytes ($r^2 = 0.50$, $p < 0.001$) prymnesiophytes ($r^2 = 0.37$, $p < 0.01$), chl *a* ($r^2 = 0.33$, $p < 0.01$), DMS yield from $DMSP_d$ ($r^2 = 0.32$, $p < 0.01$), and bacteria ($r^2 = 0.25$, $p < 0.01$). According to these results, the PC1 is primarily influenced by microbial DMSP cycling variables as well as phytoplankton-related variables. The main variables that significantly contribute to the formation of the PC2 are latitude ($r^2 = 0.68$, $p < 0.001$), water temperature ($r^2 = 0.57$, $p < 0.001$), $NO_3^- + NO_2^-$ ($r^2 = 0.53$, $p < 0.001$), cryptophytes ($r^2 = 0.48$ $p < 0.001$), incident PAR ($r^2 = 0.34$, $p < 0.01$), salinity ($r^2 = 0.33$, $p < 0.01$), DMS ($r^2 = 0.31$, $p < 0.01$) and SML depth ($r^2 = 0.25$, $p < 0.01$). These contributions suggest that PC2 mostly represents environmental forcings along with concentrations of DMS and cryptophytes.

Discussion

Spatial and seasonal variations in oceanographic conditions

In this study we captured and followed the seasonal and meridional development of the annual phytoplankton bloom as well as the associated changes in the distribution of methylated S compounds. Our dataset covered various trophic regimes commonly encountered in oceanic regions, from the oligotrophic waters of the subtropical gyre, to sub-Arctic waters, crossing the more productive waters at mid-latitude (Figs. 2; 3). Low-latitude stations located in the subtropical provinces Gulf stream, North Atlantic Subtropical Gyre West and East (GFST, NASE and NASW) displayed low sea surface concentrations of $NO_3^- + NO_2^-$ (<2.0 μmol l^{-1}) and chl *a* (<0.5 μg l^{-1}) throughout the seasons investigated, a feature commonly observed among oligotrophic systems (Williams and Follows 2003). Mid-latitude stations located in temperate and subarctic provinces (stations ranging roughly from 45 to 55°N), exhibited characteristic springtime nutrient maxima (Fig. 2c), followed by a typical summer drawdown (Williams and Follows 2003). The exception to this trend occurred in the Northwest Continental Shelves (NWCS) province (Station L) during spring, which had already experienced nutrient depletion following the onset and decline of the spring diatom bloom (Lizotte et al. 2008). Nutrient concentrations at high-latitude stations (above 55°N) during summer and fall remained near the lower range of concentrations typically found in winter for the subarctic N Atlantic

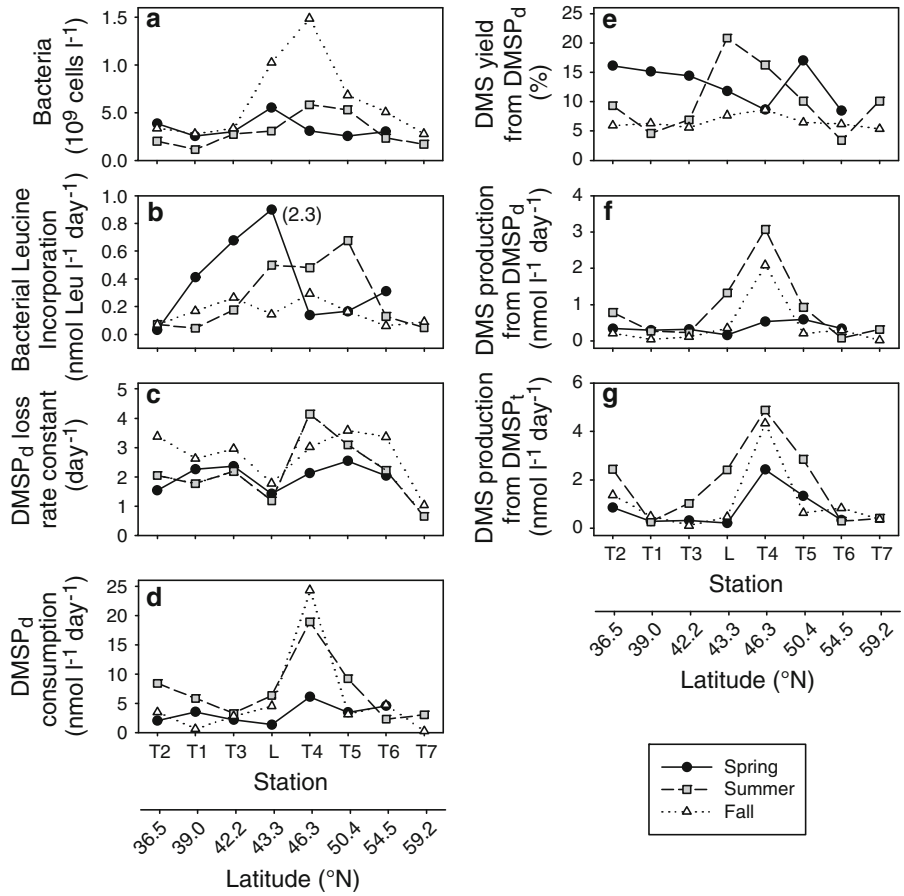

Fig. 5 Spatio-temporal variations of **a** bacterial abundance, **b** bacterial leucine incorporation, **c** $DMSP_d$ loss rate constant, **d** $DMSP_d$ consumption, **e** DMS yield from $DMSP_d$, **f** net DMS production from $DMSP_d$, and **g** net DMS production from $DMSP_t$ estimated at one depth (8–15 m) in the SML. Note that the value for bacterial leucine incorporation at Station T3 in spring was measured at 10 m, instead of 15 m like the other variables for this station during this season

($NO_3^- + NO_2^- > 5$ µmol l^{-1}) suggesting that light limitation of primary producers due to deeper mixed layers may have limited the consumption of nutrients by algae (Miller 2004 and references therein).

The distribution of the phytoplankton taxonomic groups shows the expected diatom bloom and associated macronutrient drawdown at T3 in spring and its northward progression to T4 in summer (Fig. 3a). Chl *a* concentrations were influenced by the diatom bloom, but not totally dependent on it. Indeed, chl *a* concentrations were always high at T4 in the NADR (Fig. 2d), even in spring before the occurrence of the diatom bloom. During this first cruise, as well as the following ones, the phytoplankton community at T4 was numerically dominated by flagellates (Fig. 3d). These results show that the diatom bloom was preceded by a flagellate bloom in this part of the NADR. As discussed later, this has important consequences for the production of DMS since most of the DMSP was associated with the nanoflagellate community thriving in this province of the NW Atlantic.

DMSP distribution: importance of phytoplankton community structure

Key eukaryotic groups, identified within this study, largely influenced the distribution of DMSP across seasons and provinces in the NW Atlantic Ocean (Fig. 6). Taken as a whole, the distribution of $DMSP_p$ was broadly related to the abundance of several phytoplankton groups. Spearmans's rank correlation analyses reveal strong associations between concentrations of $DMSP_p$ and the abundance of dinoflagellates, prymnesiophytes, flagellates, and prasinophytes

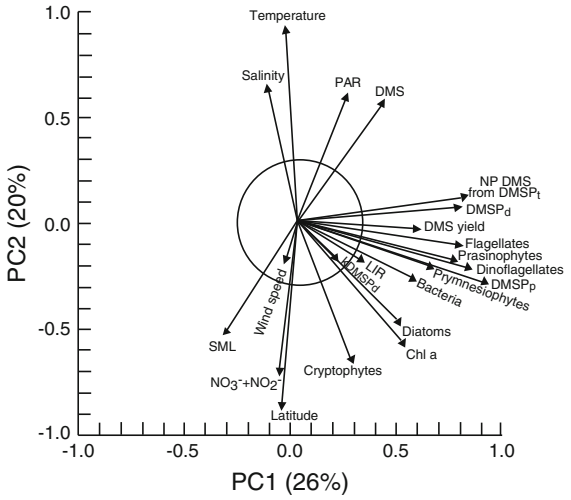

Fig. 6 PCA of 22 variables measured along a meridional transect in the NW Atlantic Ocean in spring, summer and fall 2003. The data matrix includes DMSP microbial cycling variables ($DMSP_p$, $DMSP_d$, DMS, $DMSP_d$ loss rate constant (k_{DMSPd}), DMS yield from $DMSP_d$, and NP of DMS from $DMSP_t$), biological variables (bacterial abundance and LIR, abundance of phytoplankton groups and chl *a* concentration) and environmental variables (wind speed, incident PAR, SML depth, water temperature, salinity, $NO_3^- + NO_2^-$ concentration and latitude). The *circle* of EDC is drawn

($r_s = 0.77$, $p < 0.001$; $r_s = 0.74$, $p < 0.001$; $r_s = 0.63$, $p < 0.01$ $r_s = 0.59$, $p < 0.01$, respectively). It is worth mentioning that accounting for picophytoplankton, a fraction that the microscopic cell count technique used in this study poorly characterizes, as well as using a descriptor such as carbon biomass (not available in this study) instead of cell abundance would have likely improved the relationships described between pools of $DMSP_p$ and phytoplankton taxa. For instance, picophytoplankton may dominate photosynthetic biomass in meso- to oligotrophic waters, and small prymnesiophytes (<2–3 μm) may account for a large fraction of picoeukaryotic biomass in marine ecosystems, thus potentially making a significant contribution to $DMSP_p$ pools (Archer et al. 2011; Cuvelier et al. 2010; Vaulot et al. 2008). Within the classes Dinophyceae and Prymnesiophyceae, two functional groups were shown to regularly dominate the assemblage throughout seasons: (1) dinoflagellates of the Gymnodiniales order such as species of the *Gyrodinium–Gymnodinium* complex, *Gyrodinium flagellare*, as well as *Amphidinium* ef. *kesslitzii* and (2) prymnesiophytes such as *Chrysochromulina* spp. and *Emiliania Huxleyi* (data not shown). The co-occurrence of *Chrysochromulina* spp. and *G. flagellare*, both known for their elevated DMSP quotas (Keller et al. 1989), has been previously reported in field observations and shown to coincide with high levels of DMSP and/or DMS (Cantin et al. 1996; Levasseur et al. 1996, 2004; Scarratt et al. 2002). Our results extend these previous observations and suggest that *Chrysochromulina* spp. and *G. flagellare* may represent critical players in the distribution of $DMSP_p$ from spring to fall in many biogeochemical provinces of the NW Atlantic Ocean.

In this study, spring concentrations of $DMSP_p$ (8–67 nmol l^{-1}, Fig. 4a) were similar to ranges of $DMSP_p$ concentrations previously reported within various biogeochemical provinces of the western and eastern regions of the N Atlantic Ocean during spring (9–79 nmol l^{-1} in Scarratt et al. 2000b; 3–111 nmol l^{-1} in Andreae et al. 2003). At the low-latitude oligotrophic stations, concentrations of $DMSP_p$ displayed little seasonal variability, which contrasts with temporal studies that have observed high concentrations of $DMSP_p$ in association with spring blooms in oligotrophic regions such as the Sargasso Sea (Dacey et al. 1998) and the Mediterranean Sea (Vila-Costa et al. 2008). In general, the highest concentrations of $DMSP_p$ (up to 101 nmol l^{-1}) and highest ratios of $DMSP_p$:chl *a* (mean of 72 nmol μg^{-1} in summer compared to 21 and 38 nmol μg^{-1} during spring and fall, respectively) were observed during summer, a pattern that is consistent with seasonal observations from Vila-Costa et al. (2008). Although few studies report on fall distributions of $DMSP_p$, the range of $DMSP_p$ concentrations observed in the present study (4–63 nmol l^{-1}, Fig. 4a) is similar to the range (10–46 nmol $DMSP_p$ l^{-1}) observed in fall by Scarratt et al. (2007) in surface waters of subtropical to polar regions of the NW Atlantic Ocean.

Regardless of the season, $DMSP_p$ concentrations were at their highest at mid-latitude stations located within the NADR province (Fig. 4a) which also displayed high concentrations of chl *a* and DMSP-rich phytoplankton (Fig. 2d; Fig. 3). This result provides further support to the suggestion that the NADR province, which is physically dynamic due to the convergence of warm waters of the GFST and cold polar waters (Clarke et al. 1980), may promote mixing and a concurrent flux of nutrients which may favor the growth of a mixed phytoplankton assemblage, including both $DMSP_p$-rich and $DMSP_p$-poor phytoplankton groups (Fig. 3), as evidenced by the mid-range values

of chl *a* specific DMSP reported in this region (average of 54 ± 4 nmol μg^{-1} at T4). Observations of a relative "hotspot" for concentrations of $DMSP_p$ during spring in the NADR province have been reported before (Scarratt et al. 2000b, 2002; Levasseur et al. 2004). Results from the present study show that this may be a recurrent feature that persists throughout the growing season, from the onset of a spring bloom of flagellates and its persistence until the end of October.

DMSP cycling and DMS production: importance of food web processes

We further assessed whether the macroscale features observed in the distribution of phytoplankton and DMSP may translate into variations in microbial DMSP metabolism and DMS production. Since these parameters vary at shorter time scales (hours–days) as compared to variations in phytoplankton community and $DMSP_p$ (days–weeks), we will restrict our discussion to the large recurring patterns along with the highly significant correlations that meet the threshold criteria of $p < 0.01$.

Rates of $DMSP_d$ consumption (0.3–24.3 nmol $DMSP_d$ l^{-1} day^{-1}) were comparable to those reported in other studies that employed non-perturbing additions of ^{35}S-DMSP: 2–59 nmol $DMSP_d$ l^{-1} day^{-1} in oceanic and shelf sites of the Northern Gulf of Mexico in September (Kiene and Linn 2000a); 8–30 nmol $DMSP_d$ l^{-1} day^{-1} during a Lagrangian study in the N Sea in June (Zubkov et al. 2002); 2–24 nmol $DMSP_d$ l^{-1} day^{-1} in a coastal site of the Mediterranean Sea over an annual cycle (Vila-Costa et al. 2008). The rates were generally lower than 9 nmol $DMSP_d$ l^{-1} day^{-1} and fairly constant except at T4 where the highest rates of $DMSP_d$ consumption during summer and fall were measured (19 and 24 nmol $DMSP_d$ l^{-1} day^{-1}, respectively, Fig. 5d). Only a system with a fast turnover of its DMSP reservoir could sustain such a high $DMSP_d$ consumption rate. Indeed $DMSP_d$ turnover times of 6 and 8 h were measured at Station T4 in summer and fall, respectively, reinforcing the idea that this province is very dynamic in terms of DMSP cycling.

Rates of $DMSP_d$ consumption exhibited a significant positive correlation with concentrations of $DMSP_p$ ($r_s = 0.89$, $p < 0.001$, also see Fig. 6). This result suggests that the presence of higher concentrations of $DMSP_p$ may also result in a greater availability of $DMSP_d$ to the microbial community, through the release of cellular DMSP in the water column via exudation and autolysis of the algal cells, as well as viral- and grazer-induced lysis of DMSP-containing phytoplankton (Dacey and Wakeham 1986; Hill et al. 1998). Because bacterial populations likely dominate $DMSP_d$ uptake in the oceans due to their high affinity uptake system (Kiene et al. 1998), we looked for a relationship between microbial consumption of $DMSP_d$ and bacterial production. Such a relationship had been observed in a study conducted in the Gulf of Mexico during fall (Kiene and Linn 2000a). We did not find any significant relationships between consumption of $DMSP_d$ and leucine uptake nor abundance of bacteria which suggests that, on the spatio-temporal scale considered, factors affecting the growth of bacteria (substrate availability and temperature), and the size of the population (grazing) might not affect rates of microbial $DMSP_d$ uptake. Furthermore, whilst $DMSP_d$ uptake and degradation may be prevalent among different bacterial clades (Kiene and Linn 2000a; Todd et al. 2009), it is not as widespread as leucine uptake (Vila-Costa et al. 2007), thus making its connection with bulk microbial abundance and activity not a straightforward undertaking. At the coarser scales investigated in the present study, results obtained suggest that it is the availability of DMSP which exerts the greatest influence on the overall microbial consumption of $DMSP_d$.

The proportion of $DMSP_d$ consumed by bacteria and cleaved into volatile DMS (DMS yield from $DMSP_d$) exhibited seasonal and spatial variability (mean 10%, range 3–21%; Fig. 5e). These values are remarkably similar to the average and range of values (10 and 2–21%, respectively) observed by Kiene and Linn (2000b) in various oceanic and coastal sites as well as to the annual average of 12% obtained by Vila-Costa et al. (2008) at a coastal site in the Mediterranean Sea. This finding supports the view that biological $DMSP_d$ turnover in the pelagic environment results predominantly (>79% in the present study) in other transformation pathways (including the incorporation of S into bacterioplankton) rather than in the production of DMS. A significant positive correlation was found between DMS yield from $DMSP_d$ and concentrations of $DMSP_p$ ($r_s = 0.53$, $p < 0.01$, also see PCA in Fig. 6) suggesting that there is an association between the presence of the producers of DMSP along with its release rate into the environment and the relative proportioning of microbial $DMSP_d$ transformation pathways (cleavage into DMS vs demethylation into MeSH). It cannot be excluded,

however, that the correlation found between the $DMSP_d$-to-DMS conversion efficiency and $DMSP_p$ could also partly reflect the activity of free algal DMSP-lyases in solution following manipulation during the incubations (Stefels et al. 2007). Overall, our results agree with the suggestion that substrate availability may cause shifts in the microbial-mediated degradation of $DMSP_d$ (Kiene and Linn 2000b) with higher DMSP concentrations favoring the production of volatile DMS rather than the bacterial assimilation of S.

Rates of DMS production from reservoirs of both $DMSP_d$ and $DMSP_t$ exhibited remarkable similarity in spatio-temporal patterns (Fig. 5f, g). DMS production from $DMSP_d$, ranged between 0.01 and 3.07 nmol DMS l^{-1} day^{-1} (Fig. 5f), values that are comparable to the lower range of previously reported estimates: 0.07–2.40 nmol DMS l^{-1} day^{-1} in the NW Atlantic Ocean during spring (Merzouk et al. 2008), and 0.17–5.90 nmol DMS l^{-1} day^{-1} in shelf and oceanic sites of the Northern Gulf of Mexico (Kiene and Linn 2000a). Rates of net DMS production from $DMSP_t$ obtained in the present study, from 0.12 to 4.88 nmol DMS l^{-1} day^{-1} (Fig. 5g), also compare well with the lower end of a general range of gross DMS production rates, from 0.3 to 10 nmol DMS l^{-1} day^{-1}, compiled by Simó (2004). Considering that the latter do not include DMS consumption it is expected that gross rates of DMS production be higher or equal to net rates of DMS production. Highest rates of net DMS production from $DMSP_t$ were found in the NADR province during spring, summer and fall (Fig. 5f, g) revealing yet another dynamic feature of the active DMSP cycling in this province. Seasonal peaks in net DMS production from $DMSP_t$ at stations within the NADR province (Fig. 5g) may have resulted from enhanced food web dynamics where both bacterial and non-bacterial DMS-producing processes are heightened. This could be the result of an increase in the production of DMS by potential DMSP-lyase producing species of dinoflagellates and prymnesiophytes (Wolfe and Steinke 1996; Niki et al. 2000), which abounded at stations in the NADR (Fig. 3b, c). An enhancement of DMS production due to grazing by microzooplankton may also have occurred (Dacey and Wakeham 1986; Wolfe et al. 1994) in part through a possible predator–prey relationship between *G. flagellare* and *Chrysochromulina* spp. suggested previously in the NW Atlantic (Scarratt et al. 2002; Levasseur et al. 2004). Altogether, the strengthening of these food web processes within a dynamic plankton community could have contributed to the heightened microplankton community net DMS production observed in the NADR.

Uncoupling between the distributions of DMSP and DMS

The dataset provided by this study allowed us to explore the extent of the mismatch between the distribution of DMS and chl *a* previously reported in low latitude regions of the N Atlantic and referred to as the 'summer paradox' (Simó and Pedrós-Alió 1999). In this study, a clear uncoupling between pools of DMS and concentrations of chl *a* and DMSP, as well as with the abundance of microbiota, was revealed from a two-dimensional PCA analysis (Fig. 6). By merging results obtained from all seasons and biogeochemical provinces investigated our analysis points towards environmental variables as important drivers of DMS concentrations in the NW Atlantic Ocean. Our results show positive Spearman's rank correlations between DMS and PAR as well as between DMS and SML depth irrespective of latitude and the large variability encountered, for example, in trophic status and temperature ($r_s = 0.59$ and $r_s = -0.54$, $p < 0.01$, respectively). The relationship is strengthened when DMS is related to both variables expressed together as the SML-averaged SRD ($r_s = 0.76$, $p < 0.001$). This general feature does not seem to be restricted to low latitudes during summer. These results lend support to macroscale observations of an apparent proportionality between DMS concentrations and average daily solar radiation in the SML (Vallina and Simó 2007). There is mounting evidence suggesting that exposure of microbial communities to increased levels of solar radiation may be a key factor in controlling sea-surface DMS dynamics (Sunda et al. 2002; Simó 2004; Toole and Siegel 2004; Vallina and Simó 2007). It has been suggested that solar radiation enhancement of DMS may be related to the inhibition of bacterial activity (Herndl et al. 1993) as well as to increases in the enzymatic cleavage of DMSP into DMS by phytoplankton as part of an antioxidant system that protects cells from hazardous hydroxyl (OH) radicals under high-light stress (Sunda et al. 2002). In our study, the highest seasonal mean ratios of $DMSP_t$:chl *a*, DMS:chl *a* and $DMS:DMSP_t$ (Table 2) were found during

summer suggesting the increased presence of $DMSP_p$-rich dominated phytoplankton communities and an enhancement of the fraction of $DMSP_t$ being converted into DMS under higher doses of solar radiation (see Table 2 for seasonal average PAR and SRD), possibly through enhanced phytoplankton exudation of DMS or bacterial $DMSP_d$-to-DMS conversion efficiency. However, DMS production from both $DMSP_d$ and $DMSP_t$ normalized over bulk $DMSP_t$ concentrations (Table 2) did not exhibit a clear seasonal trend with increasing PAR or SRD in summer suggesting that a more complex web of biotic and abiotic processes results in the accumulation of DMS in highly irradiated surface waters.

Station T6 in summer is a clear example of this complexity, wherein concentrations of DMS were found to peak (11 nmol l^{-1}, Fig. 4c) despite low DMS production rates from both pools of $DMSP_d$ and $DMSP_t$ (0.08 and 0.30 nmol l^{-1} day^{-1}, respectively, Fig. 5f, g) and low DMS yield from $DMSP_d$ (3%, Fig. 5e). We can only speculate that other potential sources such as indirect production of DMS via mesozooplankton grazing (not included in our $<$210 μm incubations) coupled with subdued DMS sinks such as low daily-averaged wind speeds prevailing at this station (5 m s^{-1}) and/or negligible bacterial DMS consumption (data not available) may have allowed a transient accumulation of DMS at this station. The fact that our incubations were conducted in the dark may also represent an alternative explanation for discrepancies in production rates and concentrations of DMS. A recent comparison of simultaneous dark and natural sunlight incubations conducted in contrasting microbial communities and oceanographic conditions has suggested an enhancement of DMS under natural sunlight (Galí et al. 2011) presumably through stress-induced DMS release by phytoplankton (Toole et al. 2008; Vallina et al. 2008). Enhanced solar radiation exposure has also been suggested to cause the inhibition of bacterial S demand thus potentially affecting bacterial clades that consume DMS (Slezak et al. 2001; Toole et al. 2006). However, for the latter process to be significant, this would entail rapid recovery of bacterial DMS consumers from natural sunlight conditions during the dark incubations.

Another example of the mismatch between pools of DMS and the cycling of its precursor is apparent at station T4 where mid-ranging concentrations of DMS (average of 1.3 nmol l^{-1} at T4, compared to a low of 0.4 nmol l-1 at T4, and a high of 3.9 nmol l-1 at T6, Fig. 4c) was observed despite highest rates of $DMSP_d$ uptake (Fig. 5d) and DMS production from both pools of $DMSP_d$ and $DMSP_t$ (Fig. 5f, g). It is probable that dynamic bacterial DMS production may have been tightly coupled with similarly active bacterial DMS consumption at this station. Although the absence of measurements of the bacterial DMS consumption rates prevents us from unequivocally relating both processes, studies have suggested a strong correlation between bacterial production of DMS and its consumption (Simó et al. 1995; Wolfe et al. 1999). For example, members of the Gammaproteobacteria phylogenetic group, such as *Methylophaga* spp., have been reported to actively degrade DMS in enrichment cultures (Schäfer 2007) and to display opportunistic growth on carbon-rich substrates such as DMS found in association with a DMSP-rich phytoplankton bloom in a temperate coastal environment (Neufeld et al. 2008). Taken as a whole our findings point towards a broad spatiotemporal disparity between pools of DMS and the biological cycling of DMSP (Fig. 6), whilst a significant part of the fluctuations in DMS concentrations seems to be driven by environmental variables prevalent over the NW Atlantic.

Overall, the relationship between concentrations of DMS and SRD found during this study (Fig. 6) supports the suggestion that environmental forcings such as the SML depth and the irradiance regime play prominent roles in driving surface DMS concentrations (Simó and Pedrós-Alió 1999; Simó and Dachs 2002; Vallina and Simó 2007; Miles et al. 2009). Although a feedback loop involving microbiota-DMS-clouds-solar radiation is still under much debate (Derevianko et al. 2009), our results could be regarded as an argument in support of the CLAW hypothesis. At the seasonal scale relevant to this study, an increase in solar radiation forcing would tend to decrease mixing layer depth, driving food web structure and dynamics towards enhanced sea surface concentrations of DMS.

Summary

The PCA analysis of the NW Atlantic dataset reveals clear features of the microbial DMSP cycling-related components highlighting a striking difference between the factors that influence the distribution of DMS and its precursor DMSP (Fig. 6). Salient features of our

investigation indicate that DMSP distribution is largely associated with the abundance of key phytoplankton groups identified within this study such as dinoflagellates, prymnesiophytes, unidentified nanoflagellates and prasinophytes. Microbial transformations of DMSP, that is, its consumption by bacteria and conversion into DMS, seem to be mainly driven by the availability of this substrate. Conversely, DMS concentrations appear to be ultimately correlated with environmental forcings and particularly with the irradiance regime, a result which agrees with mounting evidence pointing towards solar radiation as an important driver of DMS dynamics (Simó and Pedrós-Alió 1999; Toole and Siegel 2004; Vallina and Simó 2007; Vila-Costa et al. 2008).

Furthermore, results from this study provide evidence of the dynamic cycling of DMSP within the NADR province, where during all three seasons investigated the highest rates of microbial $DMSP_d$ uptake, as well as the highest net DMS production rates from $DMSP_d$ and $DMSP_t$ were measured. It is interesting to note that the environmental conditions in the NADR favored a persistent bloom of flagellates to which the summer diatom bloom was superimposed. Further comprehensive information on the long term cycling of DMSP and DMS in such dynamic provinces as well as in other oceanic regions is needed to improve our understanding of how DMS-emitting systems are affected by solar radiation and physical processes within the SML. The study of these issues is fundamental in the context of global climate change as possible modifications in doses of solar radiation reaching the Earth's surface (Charlson et al. 2005 and references therein), and potential weakening of the N Atlantic Drift current (Bryden et al. 2005) may have considerable implications for marine planktonic communities and the ocean-atmosphere cycling of S compounds.

Acknowledgments The authors thank the officers, crew and fellow scientists onboard the CCGS *Hudson* and the CCGS *Martha L. Black* for their assistance during the three cruises. We are particularly grateful to S. Lessard for the enumeration and identification of phytoplankton, to H. Bussey, P. Matthews, M. Hale and K. Keats for bacterioplankton data, and to S. Roy for the coordination of the cruises. Finally, we thank two anonymous reviewers who provided highly constructive comments, which helped us to improve on the original manuscript. M. Lizotte received postgraduate scholarships from Québec-Océan and the Biology department of Laval University. This project is a contribution to the research programs of the Canadian Surface Ocean—Lower Atmosphere Study funded by the Natural Sciences and Engineering Research Council of Canada, the Canadian Foundation for Climate and Atmospheric Sciences, the Department of Fisheries and Oceans Canada and of Québec-Océan funded by the Fonds québécois de la recherche sur la nature et les technologies. Funding for participation of R. Kiene was provided by the National Science Foundation through grants OPP-0083078 and OCE 0928968.

References

Andreae MO, Crutzen PJ (1997) Atmospheric aerosols: biogeochemical sources and role in atmospheric chemistry. Science 276:1052–1058

Andreae MO, Rosenfeld D (2008) Aerosol–cloud–precipitation interactions. Part 1. The nature and sources of cloud-active aerosols. Earth Sci Rev 89:13–41

Andreae MO, Andreae TW, Meyerdierks D, Thiel C (2003) Marine sulfur cycling and the atmospheric aerosol over the springtime North Atlantic. Chemosphere 52:1321–1343

Archer SD, Smith GC, Nightingale PD, Widdicombe CE, Tarran GA, Rees AP, Burkill PH (2002) Dynamics of particulate dimethylsulphoniopropionate during a Lagrangian experiment in the northern North Sea. Deep Sea Res Part II 49:2979–2999

Archer SD, Tarran GA, Stephens JA, Butcher LJ, Kimmance SA (2011) Combining cell sorting with gas chromatography to determine phytoplankton group-specific intracellular dimethylsulfoniopropionate. Aquat Microb Ecol 62: 109–121

Bryden HL, Longworth HR, Cunningham SA (2005) Slowing of the Atlantic meridional overturning circulation at 25°N. Nature 438:655–657

Cantin G, Levasseur M, Gosselin M, Michaud S (1996) Role of zooplankton in the mesoscale distribution of surface dimethylsulfide concentrations in the Gulf of St. Lawrence. Can Mar Ecol Prog Ser 141:1–3

Charlson RJ, Lovelock JE, Andreae MO, Warren SG (1987) Oceanic phytoplankton, atmospheric sulphur, cloud albedo and climate. Nature 326:655–661

Charlson RJ, Valero FPJ, Seinfeld JH (2005) In search of balance. Science 308:806–807

Clarke RA, Hill HW, Reiniger RF, Warren BA (1980) Current system south and east of the Grand Banks of Newfoundland. J Phys Oceanogr 10:25–65

Cuvelier ML, Allen AE, Monier A, McCrow JP, Messié M, Tringe SG, Woyke T, Welsh RM, Ishoey T, Lee J-H, Binder BJ, DuPont CL, Latasa M, Guigand C, Buck KR, Hilton J, Thiagarajan M, Caler E, Read B, Lasken RS, Chavez FP, Worden AZ (2010) Targeted metagenomics and ecology of globally important uncultured eukaryotic phytoplankton. Proc Natl Acad Sci 107(33):14679–14684

Dacey JWH, Wakeham SG (1986) Oceanic dimethylsulfide: production during zooplankton grazing on phytoplankton. Science 233:1314–1316

Dacey JWH, Howse FA, Michaels AF, Wakeham SG (1998) Temporal variability of dimethylsulfide and dimethylsulfoniopropionate in the Sargasso Sea. Deep Sea Res Part I 45:2085–2104

Derevianko GJ, Deutsch C, Hall A (2009) On the relationship between ocean DMS and solar radiation. Geophys Res Lett 36:L17606. doi:10.1029/2009GL039412

Devred E, Sathyendranath S, Platt T (2007) Delineation of ecological provinces using ocean colour radiometry. Mar Ecol Prog Ser 346:1–13

Galí M, Saló V, Almeda R, Calbet A, Simó R (2011) Stimulation of gross dimethylsulfide (DMS) production by solar radiation. Geophys Res Lett 38:L15612. doi:10.1029/2011GL048051

Herndl GJ, Muller-Niklas G, Frick J (1993) Major role of ultraviolet-B in controlling bacterioplankton growth in the surface layer of the ocean. Nature 361:717–719

Hill RW, White B, Cottrell M, Dacey JWH (1998) Virus-mediated release of dimethylsulfoniopropionate from marine phytoplankton. Aquat Microb Ecol 14:1–6

Keller MD, Bellows WK, Guillard RRL (1989) Dimethyl sulfide production in marine phytoplankton. In: Saltzman ES, Cooper WJ (eds) Biogenic sulfur in the environment. American Chemical Society, Washington, DC, pp 167–182

Kiene RP, Linn LJ (2000a) Distribution and turnover of dissolved DMSP and its relationship with bacterial production and dimethylsulfide in the Gulf of Mexico. Limnol Oceanogr 45:849–861

Kiene RP, Linn LJ (2000b) The fate of dissolved dimethylsulfoniopropionate (DMSP) in seawater: tracer studies using ^{35}S-DMSP. Geochim Cosmochim Acta 64:2797–2810

Kiene RP, Slezak D (2006) Low dissolved DMSP concentrations in seawater revealed by small-volume gravity filtration and dialysis sampling. Limnol Oceanogr Methods 4:80–95

Kiene RP, Hoffman Williams LP, Walker JE (1998) Seawater microorganisms have a high affinity glycine betaine uptake system which also recognizes dimethylsulfoniopropionate. Aquat Microb Ecol 15:39–51

Kiene RP, Linn LJ, Bruton JA (2000) New and important roles for DMSP in marine microbial communities. J Sea Res 43:209–224

Kirchman DL, Ducklow HW (1993) Estimating conversion factors for the thymidine and leucine methods for measuring bacterial production. In: Kemp PF, Sherr BF, Sherr EV, Cole JJ (eds) Handbook of methods in aquatic microbial ecology. Lewis Publishers, Boca Raton, pp 513–518

Lana A, Bell TG, Simó R, Vallina SM, Ballabrera-Poy J, Kettle AJ, Dachs J, Bopp L, Saltzman ES, Stefels J, Johnson JE, Liss PS (2011) An updated climatology of surface dimethylsulfide concentrations and emission fluxes in the global ocean. Glob Biogeochem Cycles 25:GB1004. doi:10.1029/2010GB003850

Legendre P, Legendre L (1998) Numerical ecology. Elsevier Science BV, Amsterdam

Levasseur M, Michaud S, Egge J, Cantin G, Nejstgaard JC, Sanders R, Fernandez E, Solberg PT, Heimdal B, Gosselin M (1996) Production of DMSP and DMS during a mesocosm study of an *Emiliania huxleyi* bloom: influence of bacteria and *Calanus finmarchicus* grazing. Mar Biol 126:609–618

Levasseur M, Scarratt MG, Roy S, Laroche D, Michaud S, Cantin G, Gosselin M, Vézina A (2004) Vertically resolved cycling of dimethylsulfoniopropionate (DMSP) and dimethylsulfide (DMS) in the Northwest Atlantic in spring. Can J Fish Aquat Sci 61:744–757

Levitus S (1982) Climatological Atlas of the World Ocean, NOAA/ERL GFDL professional Paper 13. Princeton, N.J

Lizotte M, Levasseur M, Scarratt MG, Michaud S, Merzouk A, Gosselin M, Pommier J (2008) Fate of DMSP during the decline of the Northwest Atlantic spring diatom bloom. Aquat Microb Ecol 52:159–173

Longhurst A (2006) The Atlantic Ocean. In: Longhurst A (ed) Ecological geography of the sea, 2nd edn. Elsevier Science Publishers, New York, pp 131–268

Longhurst A, Sathyendranath S, Platt T, Caverhill C (1995) An estimate of global primary production in the ocean from satellite radiometer data. J Plankton Res 17:1245–1271

Lovelock JE, Maggs RJ, Rasmussen RA (1972) Atmospheric dimethyl sulphide and the natural sulphur cycle. Nature 237:452–453

Malmstrom RR, Kiene RP, Vila M, Kirchman DL (2005) Dimethylsulfoniopropionate (DMSP) assimilation by *Synechococcus* in the Gulf of Mexico and northwest Atlantic Ocean. Limnol Oceanogr 50:1924–1931

Merzouk A, Levasseur M, Scarratt M, Michaud S, Lizotte M, Rivkin RB, Kiene RP (2008) Bacterial DMSP metabolism during the senescence of the spring diatom bloom in the Northwest Atlantic. Mar Ecol Prog Ser 369:1–11

Michaud S, Levasseur M, Cantin G (2007) Seasonal variations in dimethylsulfoniopropionate and dimethylsulfide concentrations in relation to the plankton community in the St. Lawrence Estuary. Estuar Coast Shelf Sci 71:741–750

Miles CJ, Bell TG, Lenton TM (2009) Testing the relationship between the solar radiation dose and surface DMS concentrations using in situ data. Biogeosciences 6:1927–1934

Miller CB (2004) Biological oceanography. Blackwell Publishing, Oxford

Neufeld JD, Boden R, Moussard H, Schäfer H, Murrell C (2008) Substrate-specific clades of active marine methylotrophs associated with a phytoplankton bloom in a temperate coastal environment. Appl Environ Microbiol 74(23):7321–7328

Niki T, Kunugi M, Otsuki A (2000) DMSP-lyase activity in five marine phytoplankton species: its potential importance in DMS production. Mar Biol 136:759–764

Parsons TR, Maita Y, Lalli CM (1984) A manual of chemical and biological methods for seawater analysis. Pergamon Press, Oxford

Platt T, Sathyendranath S (1999) Spatial structure of pelagic ecosystem processes in the global ocean. Ecosystems 2:384–394

Pommier J, Michel C, Gosselin M (2008) Particulate organic carbon export in the upper twilight zone during the decline of the spring bloom. Mar Ecol Prog Ser 356:81–92

Porter KG, Feig YS (1980) The use of DAPI for identifying and counting aquatic microflora. Limnol Oceanogr 25:943–948

Scarratt MG, Cantin G, Levasseur M, Michaud S (2000a) Particle size-fractionated kinetics of DMS production: where does DMSP cleavage occur at the microscale? J Sea Res 43:245–252

Scarratt MG, Levasseur M, Schultes S, Michaud S, Cantin G, Vézina A, Gosselin M, de Mora SJ (2000b) Production and consumption of dimethylsulfide (DMS) in North Atlantic waters. Mar Ecol Prog Ser 204:13–26

Scarratt MG, Levasseur M, Michaud S, Cantin G, Gosselin M, de Mora SJ (2002) Influence of phytoplankton taxonomic profile on the distribution of dimethylsulfide and dimethylsulfoniopropionate in the northwest Atlantic. Mar Ecol Prog Ser 244:49–61

Scarratt MG, Levasseur M, Michaud S, Roy S (2007) DMSP and DMS in the Northwest Atlantic: late-summer distributions, production rates and sea-air fluxes. Aquat Sci 69:292–304

Schäfer H (2007) Isolation of *Methylophaga* spp. from marine dimethylsulfide-degrading enrichment cultures and identification of polypeptides induced during growth on dimethylsulfide. Appl Environ Microbiol 73(8):2580–2591

Simó R (2001) Production of atmospheric sulfur by oceanic plankton: biogeochemical, ecological and evolutionary links. Trends Ecol Evol 16:287–294

Simó R (2004) From cells to globe: approaching the dynamics of DMS(P) in the ocean at multiple scales. Can J Fish Aquat Sci 61:673–684

Simó R, Dachs J (2002) Global ocean emission of dimethylsulfide predicted from biogeophysical data. Glob Biogeochem Cycles 16(4):1018. doi:10.1029/2001GB001829

Simó R, Pedrós-Alió C (1999) Role of vertical mixing in controlling the oceanic production of dimethyl sulphide. Nature 402:396–399

Simó R, Grimalt JO, Pedrós-Alió C, Albaigés J (1995) Occurrence and transformation of dissolved dimethyl sulfur species in stratified seawater (western Mediterranean Sea). Mar Ecol Prog Ser 127:291–299

Slezak D, Brugger A, Herndl GJ (2001) Impact of solar radiation on the biological removal of dimethylsulfoniopropionate and dimethylsulfide in marine surface waters. Aquat Microb Ecol 25:87–97

Slezak D, Kiene RP, Toole DA, Simó R, Kieber DJ (2007) Effects of solar radiation on the fate of dissolved DMSP and conversion to DMS in seawater. Aquat Sci 69: 377–393. doi:10.1007/s00027-007-0896-z

Sokal RR, Rohlf FJ (1995) Biometry: the principles and practice of statistics in biological research, 3rd edn. WH Freeman and Co., New York

Stefels J (2000) Physiological aspects of the production and conversion of DMSP in marine algae and higher plants. J Sea Res 43:3–4

Stefels J, Steinke M, Turner S, Malin G, Belviso S (2007) Environmental constraints on the production and removal of the climatically active gas dimethylsulphide (DMS) and implications for ecosystem modelling. Biogeochem 83: 254–275

Sunda W, Kieber DJ, Kiene RP, Huntsman S (2002) An antioxidant function for DMSP and DMS in marine algae. Nature 418:317–320

Todd JD, Curson ARJ, Dupont CL, Nicholson P, Johnston AWB (2009) The dddP gene, encoding a novel enzyme that converts dimethylsulfoniopropionate into dimethyl sulphide, is widespread in ocean metagenomes and marine bacteria and also occurs in some Ascomycete fungi. Environ Microbiol 11:1376–1385

Toole DA, Siegel DA (2004) Light-driven cycling of dimethylsulfide (DMS) in the Sargasso Sea: closing the loop. Geophys Res Lett 31:L09308. doi:10.1029/2004GL019581

Toole DA, Slezak D, Kiene RP, Kieber DJ, Siegel DA (2006) Effects of solar radiation on dimethylsulfide cycling in the western Atlantic Ocean. Deep Sea Res Part I 53:136–153

Toole DA, Siegel DA, Doney SC (2008) A light-driven one-dimensional dimethylsulfide biogeochemical cycling model for the Sargasso Sea. J Geophys Res 113:G02009. doi:10.1029/2007JG000426

Utermöhl H (1931) Neue wege in der quantitativen erfassung des planktons (mit besonderer berücksichtigung des ultraplanktons). Verh Int Ver Theor Angew Limnol 5:567–596

Vallina SM, Simó R (2007) Strong relationship between DMS and the solar radiation dose over the global surface ocean. Science 315:506–508

Vallina SM, Simó R, Anderson TR, Gabric A, Cropp R, Pacheco JM (2008) A dynamic model of oceanic sulfur (DMOS) applied to the Sargasso Sea: Simulating the dimethylsulfide (DMS) summer paradox. J Geophys Res 113:G01009. doi: 10.1029/2007JG000415

Vaulot D, Eirem W, Viprey M, Moreau H (2008) The diversity of small eukaryotic phytoplankton (<3 μm) in marine ecosystems. FEMS Microbiol Rev 32:795–820

Vila-Costa M, Simó R, Harada H, Gasol JM, Slezak D, Kiene RP (2006) Dimethylsulfoniopropionate uptake by marine phytoplankton. Science 314:652–654

Vila-Costa M, Pinhassi J, Alonso C, Pernthaler J, Simó R (2007) An annual cycle of dimethylsulfoniopropionate-sulfur and leucine assimilating bacterioplankton in the coastal NW Mediterranean. Environ Microbiol 9:2451–2463

Vila-Costa M, Kiene RP, Simó R (2008) Seasonal variability of the dynamics of dimethylated sulfur compounds in a coastal northwest Mediterranean site. Limnol Oceanogr 53:198–211

Williams RG, Follows MJ (2003) Physical transport of nutrients and the maintenance of biological production. In: Fasham MJR (ed) Ocean biogeochemistry: the role of the ocean carbon cycle in global change. Global Change-The IGBP series, Springer-Verlag

Wolfe GV, Steinke M (1996) Grazing-activated production of dimethyl sulfide (DMS) by two clones of *Emiliania huxleyi*. Limnol Oceanogr 41:1151–1160

Wolfe GV, Sherr EB, Sherr BF (1994) Release and consumption of DMSP from *Emiliania huxleyi* during grazing by *Oxyrrhis marina*. Mar Ecol Prog Ser 111:111–119

Wolfe GV, Levasseur M, Cantin G, Michaud S (1999) Microbial consumption and production of dimethyl sulfide (DMS) in the Labrador Sea. Aquat Microb Ecol 18:197–205

Yoch DC (2002) Dimethylsulfoniopropionate: its sources, role in the marine food web, and biological degradation to dimethylsulfide. Appl Environ Microbiol 68:5804–5815

Zubkov MV, Fuchs BM, Archer SD, Kiene RP, Amann R, Burkill PH (2002) Rapid turnover of dissolved DMS and DMSP by defined bacterioplankton communities in the stratified euphotic zone of the North Sea. Deep Sea Res Part II 49:3017–3038